PCCP

Cite this: *Phys. Chem. Chem. Phys.*, 2012, **14**, 3589–3595

www.rsc.org/pccp

PAPER

The degradation mechanism of methyl orange under photo-catalysis of TiO_2†

Lihong Yu,[a] Jingyu Xi,[b] Ming-De Li,[a] Hung Tat Chan,[a] Tao Su,[a] David Lee Phillips*[a] and Wai Kin Chan*[a]

Received 13th October 2011, Accepted 3rd January 2012
DOI: 10.1039/c2cp23226j

The properties of photo-generated reactive species, holes and electrons in bulk TiO_2 (anatase) film and nano-sized TiO_2 were studied and their effects towards decomposing pollutant dye methyl orange (MO) were compared by transient absorption spectroscopies. The recombination of holes and electrons in nano-sized TiO_2 was found to be on the microsecond time scale consistent with previous reports in the literature. However, in bulk TiO_2 film, the holes and electrons were found to be on the order of picoseconds due to ultra fast free electrons. The time-correlated single-photon counting (TCSPC) technique combined with confocal fluorescence microscopy revealed that the fluorescence intensity of MO is at first enhanced noticeably by TiO_2 under UV excitation and soon afterwards weakened dramatically, with the lifetime prolonged. Photo-generated holes in nano-sized TiO_2 can directly oxidize MO on the time scale of nanoseconds, while free electrons photo-generated in bulk TiO_2 film can directly inject into MO on the order of picoseconds. Through cyclic voltammetry measurements, it was found that MO can be reduced at −0.28 V and oxidized at 1.4 V (*vs.* SCE) and this provides thermodynamic evidence for MO to be degraded by electrons and holes in TiO_2. Through comparison of the hole-scavenging effect of MO and water, it was found that in polluted water when MO is above 1.6×10^{-4} M, the degradation is mainly due to a direct hole oxidation process, while below 1.6×10^{-4} M, hydroxyl oxidation competes strongly and might exceed the hole oxidation.

Introduction

TiO_2 has found many industrial applications as a photocatalyst for degradation of organic pollutants or in solar energy conversion devices[1–5] because of its efficient photo-activity, high stability, low cost and being relatively safe toward humans and the environment. Among environmental pollutants, azo-dyes including methyl orange (MO) make up a significant component of organic pollutants in general. Azo-dyes like methyl orange have many undesirable consequences on ecosystems affected by them. Much work has been spent on investigating the decomposition of azo-dyes using TiO_2 and great progress has been made since the 1980s.[6] A better understanding of the mechanism for the photo-catalytic reactions of TiO_2 is extremely important for improving the degradation efficiency and rate for practical applications. Due to the contributions of many researchers over the past three decades, the primary steps occurring in photo-catalytic degradation can be summarized as follows.[2,7–9] Firstly, electrons and holes are photo-induced in the valence band and conduction band of TiO_2 respectively. Some of these electrons and holes can then escape direct recombination to reach the surface of TiO_2 so as to react with hydroxyl groups or water to form $OH^{\bullet}$ radicals that have a high reactivity toward decomposing organic compounds like azo-dyes. In addition, a minor amount of other oxidative species, such as $O_2^{\bullet -}$ and H_2O_2, can be generated through the capture of electrons in the conduction band.[10–13] It is generally believed that the degradation of pollutant dyes is mainly based on the production of the hydroxyl radicals ($HO^{\bullet}$).[6,14–16] However, some controversy still exists and the major uncertainty appears to be whether oxidation reactions proceed *via* direct electron transfer between the organic pollutants and TiO_2 or *via* an $OH^{\bullet}$ radical-mediated process.

It was suggested that at the surface of TiO_2, an electron transfer from nearby dyes to TiO_2 holes is thermodynamically feasible[14] since the oxidation potentials of most organic compounds lie below that of the holes in the TiO_2 valence band. Usually, the photo-degradation of dyes typically takes over in tens of minutes using a heterogeneous catalyst and monitoring the bulk solution with UV-Vis spectroscopy.[17]

[a] *Department of Chemistry, The University of Hong Kong, Pokfulam Road, Hong Kong, P. R. China. E-mail: phillips@hku.hk, waichan@hku.hk*
[b] *Lab of Advanced Power Sources, Graduate School at Shenzhen, Tsinghua University, Shenzhen, P. R. China*
† Electronic supplementary information (ESI) available. See DOI: 10.1039/c2cp23226j

Unfortunately, very few transient processes and short-lived species of the reactions between semiconductors and dyes have been reported. Nowadays, with the development of ultrafast and fast photochemistry instrumentation, it is possible and feasible to observe the transient reaction of electrons and holes with the surrounding pollutant dyes in order to gain a better understanding of the degradation reaction mechanisms. In this study, we used methyl orange (MO) as a model dye since it has often been used as a model dye to probe the photo degradation chemistry occurring on semiconductor particles.[18] The different recombination rates of the holes and electrons in bulk TiO_2 film and nano-sized TiO_2 were compared with each other and also with their different reactivity towards decomposition of MO. The direct reactions between MO molecules and holes and electrons were observed and this allows the competition between MO, water and oxygen concerning the capture of holes and electrons to be examined through highly sensitive femtosecond and nanosecond transient absorption spectroscopy and through transient fluorescence decay spectroscopy.

Experimental section

Samples

Methyl Orange (MO) was used as received commercially (ACROS organics) with pure certified grade. Anatase nano-sized TiO_2 was obtained commercially with a BET surface area of 135.8 $m^2\ g^{-1}$ and a primary diameter of 10–15 nm. For the nanosecond transient absorption (nanosecond TA) measurement, the nano-sized TiO_2 was dispersed in acetonitrile forming steady and half-transparent suspension by ultrasonication. The suspension was placed in an optical quartz cell and the pump laser and the probe light are orthogonally crisscrossing in the suspension. For the femtosecond transient absorption (femtosecond TA) measurement, the bulk TiO_2 film was prepared from the commercially available organic paste (Dyesol Australia) containing the TiO_2 nanoparticles. The TiO_2 paste was printed on a quartz substrate by a screen-printing method.[19] The sample was then heated at 500 °C for 3 hours and the opaque film became transparent with about 2 cm × 1 cm in area and 6 μm in thickness. The bulk TiO_2 film was placed in an optical quartz cell containing a solution of the reactant (MO in acetonitrile). O_2 is an electron-capturer which can produce $O_2^{\bullet -}$,[20] an important intermediate species. Therefore, to test the reaction between MO and TiO_2, N_2 was bubbled through the suspensions before nano- and femtosecond TA experiments to ensure that the samples are without appreciable O_2. For the TCSPC measurement, both the bulk TiO_2 film and nano-sized TiO_2 were used. The nano-sized TiO_2 suspension in acetonitrile was coated on a quartz substrate. After drying, an opaque but even film was formed. Finally, MO solution was spread and dried on the TiO_2 film surface for the transient fluorescence decay measurements.

Instrumentation

Transient Fluorescence Decay measurements were performed by using the Time Correlated Single-Photon Counting (TCSPC) technique with a confocal fluorescence microscope system (HORIBA, Ltd.). The excitation light source was a mode-locked Ar^+ ion laser centered at 370 nm, operated at a frequency of 8 MHz. The fluorescence photon was collected between 540 nm and 580 nm and no counts of fluorescence from the TiO_2 or quartz substrate was detected. Cyclic Voltammetry (CV) experiments were conducted on a PARSTAT 2273 Advanced Electrochemical System using SCE as the reference electrode. The solution of MO in CV experiments was about 10^{-3} M with KCl as conduction electrolyte. The nanosecond TA experiment was carried out using a LP920 laser flash spectrometer manufactured by Edinburgh Instruments Ltd. The probe light source was a 450 W ozone free Xe arc lamp producing a continuous spectrum between 150 and 2600 nm. The pump light was generated by a Q-switched Nd:YAG laser (Model: Lab 150-10 4056L; 3rd harmonic line at λ = 355 nm). The TA signal was recorded with a TDS 3012C digital signal analyzer. The femtosecond TA experiment was carried out by a femtosecond Ti:Sapphire regenerative amplified Ti:Sapphire laser system (Spectra Physics, Spitfire-Pro) and an automated data acquisition system (Ultrafast Systems, Helios). The pump laser was of 267 nm (the third harmonic of the fundamental 800 nm from the regenerative amplifier). The probe pulse was white-light continuum (450–800 nm) generated by a sapphire plate using approximately 5% of the original output from the Spitfire. Before passing through the sample the probe pulse was split into two beams: one beam travels through the sample, and the other is sent directly to a reference spectrometer that monitors the fluctuation of the probe beam intensity. The instrument response function is evaluated to be 150 fs. The TA signals of all samples in the nanosecond TA experiment and the femtosecond TA experiment with the occurrence of the photo-catalytic reactions were reproducible, and therefore the accumulation of photo-catalytic products was negligible.

Results and discussion

Transient fluorescence decay study

UV-Vis absorption and fluorescence emission spectra of MO are shown in ESI† (see Fig. S1). The UV-Vis absorption spectrum of MO is consistent with those previously reported in the literature[15] and there is no appreciable absorption of MO beyond 570 nm up to the 800 nm spectral region examined here. In the fluorescence emission spectrum (see Fig. S1 (ESI†), solid), MO emits fluorescence photons between 480 nm and 650 nm with a maximum at around 560 nm. Fig. 1 shows the fluorescence decay profiles of MO adsorbed on quartz, bulk TiO_2 film and nano-sized TiO_2, respectively, unnormalized in (a) and normalized in (b). In a typical electron transfer process from a dye (for example N719) to anatase TiO_2 under UV excitation, the fluorescence intensity of the dye is usually quenched meanwhile with its lifetime shortened to some extent. This can be observed by transient fluorescence decay measurement through the TCSPC technique.[21] However, in our experiment, the fluorescence of MO is not quenched by TiO_2 after UV excitation, and instead the fluorescence intensity is enhanced and its lifetime becomes slightly longer as shown in Fig. 1(a) and (b). Fig. 1(a) indicates that within the same measuring time, the fluorescence intensity of MO dye on bulk TiO_2 film and the nano-sized TiO_2 is much higher than that acquired on quartz. Whether this observation is mainly due to that TiO_2 acts as a photonic crystal (PC)[22] (which leads to enhanced emission intensity

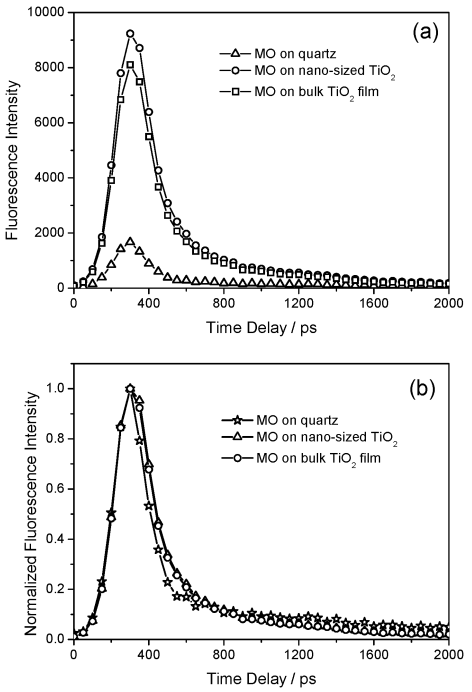

Fig. 1 (a) Fluorescence decay profiles by TCSPC of MO adsorbed on quartz, bulk TiO_2 film and nano-sized TiO_2 respectively. (b) The normalization of the fluorescence decay profiles of (a). For samples preparation, 0.1 millimetre of 4×10^{-4} M MO solution is spread, respectively, on the surface of quartz, bulk TiO_2 film and nano-sized TiO_2 and then dried and the unadsorbed MO on TiO_2 is rinsed off. The detected area is 10 μm in diameter where the MO layer is spread homogeneously under a microscope. Time taken for each measuring process is 50 s.

of some organic dyes) or that electrons are transferred from the TiO_2 conduction band to the MO excited state (which may enhance emission intensity of MO) was not determined here. However, after normalization (see Fig. 1(b)), the decay profiles of MO on the bulk TiO_2 film and the nano-sized TiO_2 nearly overlap with each other and both of them are close to that of MO on quartz. This suggests that the lifetime of the MO fluorescence had no significant change when adsorbed on TiO_2 and excited by the UV laser for a short time like 50 s. The fluorescence decay profile of MO on quartz can be fitted well with a two-exponential function. The fast decay time constant is 117 ps (86%) and the slow decay time constant is 3.09 ns (14%). However, the fluorescence decay profiles of MO on the bulk TiO_2 film and the nano-sized TiO_2 could not be fitted by multi-exponential functions. This suggests that some reaction happened between MO and TiO_2. Even though their precise decay time constants remain difficult to extract, it is easily found that in the fast decay part of the profiles, the fluorescence decay of MO on the bulk TiO_2 film and the nano-sized TiO_2 substrates is slower than that of the corresponding component on the quartz substrate. In other words, the fluorescence lifetime of MO appears to be prolonged slightly. This probably implies that the electrons on the excited states of MO would not transfer to the conduction band of TiO_2.

In aqueous solution, MO has been suggested to be decomposed by hydroxyl radicals $HO^{\bullet}$ through TiO_2 catalysis under UV excitation.[14–16] Fig. 2 shows fluorescence decay profiles of MO on bulk TiO_2 film (a), on nano-sized TiO_2 (c), and on quartz (e), with measurement sequence for the same detected site. (b) and (d) are normalized decay profiles, and (f) fluorescence band intensity as a function of measurement sequence for MO on bulk TiO_2 film, on nano-sized TiO_2, and on quartz respectively. In the experiments reported here, we observed that the direct reaction between MO and TiO_2 appeared to have no aid of hydroxyl radicals $HO^{\bullet}$ for most of the apparent decomposition of MO. For each sample, the measurements were conducted on the same sample site under the same experimental conditions. Therefore the intensity and lifetime of fluorescence can well represent the temporal properties of the dye. As shown in Fig. 2(a) and (c), the fluorescence intensity drops substantially with measurement sequence. Up to the eighth time, there is almost no emission either from MO on the bulk TiO_2 film or on the nano-sized TiO_2. This suggests that the MO molecules are directly decomposed by TiO_2 under laser excitation for the following two reasons. Firstly, since the surface of TiO_2 is covered by MO with no exposure to air which can generate $O_2^{\bullet-}$ on the TiO_2 surface under laser excitation, the indirect radical attack can be excluded. Secondly, when the same experimental process is conducted on the MO dye on quartz, the fluorescence intensity and lifetime did not change regardless of the UV excitation time (Fig. 2(e)). This suggests that without TiO_2 catalysis, the MO molecules are not decomposed by UV excitation and all the excited electrons return to the ground state in nanoseconds. This result is consistent with the other reports that MO is very stable toward light and difficult to oxidize.[17] The normalized fluorescence decay profiles are shown in Fig. 2(b) and (d). It is obvious that the lifetime of the fluorescence for MO is prolonged, the longer the reaction time with TiO_2. It is interesting that the most obvious change of the fluorescence lifetime takes place between the first and second reaction processes and after that there are only gradual changes. This phenomenon suggests that most of the photo-catalysis reaction of MO occurs during the first 50 s of the photo-catalysis reaction process and the new product hinders the further charge transfer between TiO_2 and MO, which consequently decreases the fluorescence intensity and increases the fluorescence lifetime.

From Fig. 2(f), it can be seen that the fluorescence intensity of MO on the bulk TiO_2 film and the nano-sized TiO_2 drops dramatically with increasing measurement sequence, while that of MO on quartz undergoes no apparent change under the same experimental conditions. This further verifies the direct chemical reaction between MO and TiO_2. Furthermore, it is easily seen that MO on the nano-sized TiO_2 decomposes faster than that on the bulk TiO_2 film. This may be due to the advantages of nano-sized TiO_2 concerning the longer separated charges (more discussion later), surface area, light absorbance and many other factors over the bulk TiO_2 film.

Electrochemical degradation study

In order to verify the charge transfer mechanism between MO and TiO_2, cyclic voltammetry (CV) was conducted to investigate the oxidation and reduction potential of MO. Fig. 3 shows the CV profiles of MO (a), and empty solution (b). An irreversible reduction peak of MO appears at −0.28 V *vs.* SCE, and an oxidation peak appears at 1.4 V *vs.* SCE. There also exists a large current background due to oxygen formation. This indicates that MO may be reduced and oxidized by the

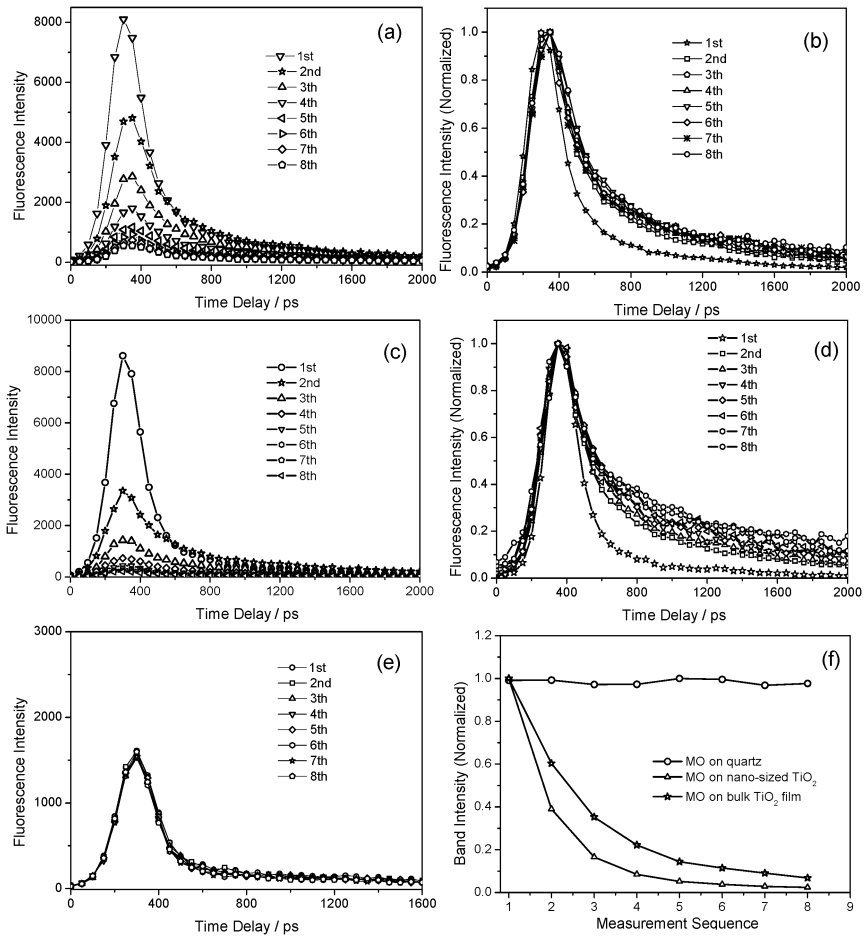

Fig. 2 Fluorescence decay profiles of MO on bulk TiO_2 film (a), on nano-sized TiO_2 (c), and on quartz (e), with different measurement sequences. For each sample, the measured position and area are unchanged. (b) and (d) Normalization profiles of (a) and (c). (f) Fluorescence band intensity in (a), (c) and (e) as a function of measurement sequence for MO on bulk TiO_2 film, on nano-sized TiO_2, and on quartz respectively. Time taken for each measuring process is 50 s.

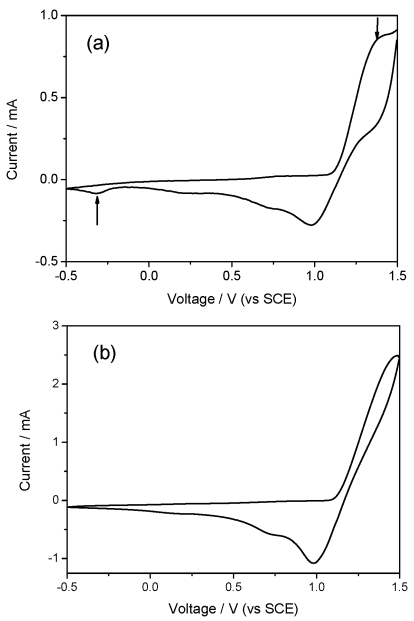

Fig. 3 CV (cyclic voltammetry) profile of 10^{-3} mol l^{-1} MO solution with 0.1 M KCl as conducting electrolyte (a), and CV profile of 0.1 M KCl solution acting as empty experiment (b). The scanning rate is 50 mV s^{-1}.

electrons and holes in TiO_2 the redox potentials of which are about −0.7 V and 2.5 V *vs.* SCE,[20] quite beyond the redox potential of MO.[23] In other words, the MO molecules tend to consume both the electrons and holes photo-induced in TiO_2.

Nanosecond TA study

It is well known that in nano-sized TiO_2, photo-generated electrons and holes recombination takes place within several microseconds. Therefore nanosecond TA experiments may be used to observe the reaction between the electrons and/or holes and MO. Acetonitrile (MeCN) is a slow hole scavenger of TiO_2 and the reaction between MeCN and holes is not detected on the microsecond time scale.[24] We used MeCN as the solvent to disperse the TiO_2 nano-particles in the nanosecond TA experiment. Fig. 4 shows the TA spectra of nano-sized TiO_2 dispersed in MeCN (a), and TA decay profiles of nano-sized TiO_2 with different concentrations of MO (b). As shown in Fig. 4(a), there is a broad TA in the visible range which is mainly assigned to holes absorption in TiO_2.[25] The precise assignment of the TA spectra of TiO_2 particles is very difficult since the electrons and holes absorption spectra are very broad and overlapping with each other, especially in the visible region.[25] It is commonly believed that in the shorter

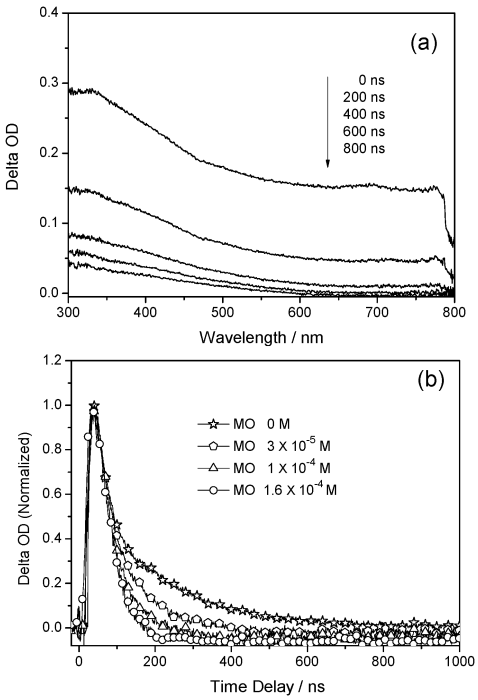

Fig. 4 TA spectra of nano-sized TiO_2 dispersed in MeCN (a), and TA decay profiles of nano-sized TiO_2 with different concentrations of MO (b). Pump by 355 nm, probe at 600 nm.

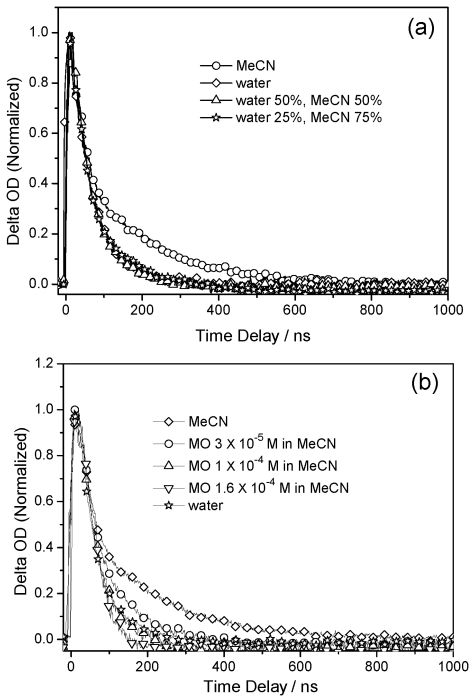

Fig. 5 TA decay profiles of nano-sized TiO_2 in a mixture of water and MeCN at different percentages (a), and TA decay profiles of nano-sized TiO_2 in MeCN with different concentrations of MO (b). Pump by 355 nm, probe at 600 nm.

wavelength range, the TA of TiO_2 is mainly due to trapped holes and weak TA of free and trapped electrons can also be detected there.[26] The TiO_2 transient absorption is sensitive to the particle size, crystal phase, and surface conditions.[27–29] Even though, by summarizing some important previous investigations,[5,25,26] general conclusions can still be made that before 750 nm, the absorption of trapped holes dominates the TA spectra and the lower the wavelength the more, while beyond 1250 nm, the absorption of free electrons dominates. In the range between 750 nm and 1250 nm, the spectra have not been assigned to a single species since the contributions of the trapped holes, trapped electrons, and free electrons are more or less the same. In fact, the spectrum of trapped electrons was only obtained by calculation instead of direct observation for it dominates no particular area in the whole spectra.[5,25,26] In Fig. 4(a), no peak is observed between 600 nm and 800 nm, suggesting that some holes are trapped evenly and shallowly which will recombine with electrons in about 800 ns, while a broad peak at about 350 nm decays more slowly, indicating that these holes are deeply trapped and they will not recombine with electrons or react with adsorbates as quickly as the shallow trapped ones. We chose 600 nm as the probe wavelength to investigate the TA dynamic for TiO_2 holes which has no overlap with the ground state absorption of MO. From Fig. 4(b), we can see that the TA decay of holes in the nano-sized TiO_2 is accelerated by MO, the more the MO the faster the decay. This suggests that MO can capture holes in TiO_2 on the nanosecond time scale. At a concentration of 1.6×10^{-4} M, the TA of the shallowly trapped holes decays to zero in less than 200 ns. Therefore the direct reaction between TiO_2 holes and MO under UV excitation is confirmed, since MeCN does not give rise to reactive intermediates like water does.

In industry, when MO is degraded in polluted water on the TiO_2 surface under sunlight, the MO concentration is often on the order of ppm. In fact, water is also a hole scavenger of TiO_2, whose product hydroxyl radicals are an effective oxidative reagent towards dyes. In order to determine whether the holes or hydroxyl radicals play a major role in MO degradation, we need to compare the reactivity of these two scavengers.

Fig. 5 shows the TA decay profiles of nano-sized TiO_2 in the mixture of water and MeCN in (a), and TA decay profiles of nano-sized TiO_2 in MeCN with different concentrations of MO in (b). From Fig. 5(a), it can be seen that in the presence of water, the TA of TiO_2 holes decays faster than in MeCN alone. It suggests that water captures the holes much faster than MeCN. The decay curves of TiO_2 with water compositions of 25, 50, and 100% have the same lifetime. As long as water is present in the solvent, its reaction rate is the same as pure water. This implies that in polluted water, no matter what concentration of MO, the production rate of hydroxyl radicals from water is the same. We compare the reactivity of water and MO in Fig. 5(b). Although the holes decay profile in water is quite similar to that in 1×10^{-4} M MO solution, it cannot be concluded that the reactivity of water capturing holes is similar to that in 1×10^{-4} M MO. On the surface of TiO_2 in acetonitrile, there are some adsorbed water molecules, which may also capture holes. However, in 1.6×10^{-4} M MO solution, the holes show a shorter lifetime than in pure water. This suggests that MO of this concentration results in a faster holes decay compared to that in pure water, since a trace amount of water adsorbed on TiO_2 would not result in a faster holes decay compared to pure water. Therefore, it is reasonable to conclude that at high MO concentration ($>1.6 \times 10^{-4}$ M), the degradation of MO is mainly due to direct hole oxidation.

In contrast, at low MO concentration ($<1 \times 10^{-4}$ M), oxidation by hydroxyl radicals may compete with direct hole oxidation.

Femtosecond TA study

In nano-sized TiO_2, the recombination of photo-generated electrons and holes occurs in several microseconds under vacuum conditions.[30] In the experiment reported here, the nano-sized TiO_2 film was heated at 500 °C for three hours and the film becomes a transparent bulk film since during the heating process the nano-sized TiO_2 has grown together forming a bulk crystal film.[31] Fig. 6 shows the femtosecond TA spectra (a) and decay profile (c) of bulk TiO_2 film, and femtosecond TA spectra (b) and decay profile (d) of MO. As shown in Fig. 6(a), the bulk TiO_2 film has two TA peaks at around 520 nm and 675 nm in the visible range. The peak at 520 nm appears sooner than the one at 675 nm, which showed up after the former one approached its maximum value. The former peak is tentatively attributed to the deeper trapped holes and the latter one to the shallow trapped holes. Their peak positions showed a slight red-shift compared to those of the nano-sized TiO_2 as shown in Fig. 4(a), probably due to the shallower trapping sites in the bulk TiO_2 film. We observed that the recombination of photo-generated electrons and holes in the bulk TiO_2 film took place in about 500 picoseconds, which is 1000 times faster than in nano-sized TiO_2 as shown in Fig. 6(c). This observation may be due to that in the bulk TiO_2 film, there are much fewer trapping sites or quantum confinement than in nano-sized TiO_2[32] and thus the generated electrons are mostly free electrons which spread all over the inner and surface areas and move ultra fast to recombine with the unmovable holes. Therefore, the faster recombination of electrons and holes in the bulk TiO_2 film is mainly due to the free electrons.

MO also has TA spectra with a peak at 520 nm (Fig. 6(b)) and its decay at 675 nm needs less than 50 ps (Fig. 6(d)), much faster than that of holes in bulk TiO_2 film. From the nanosecond TA experiment, it has already been shown that MO is not a very effective hole scavenger which consumes holes on the nanosecond time scale. This is much slower than for small

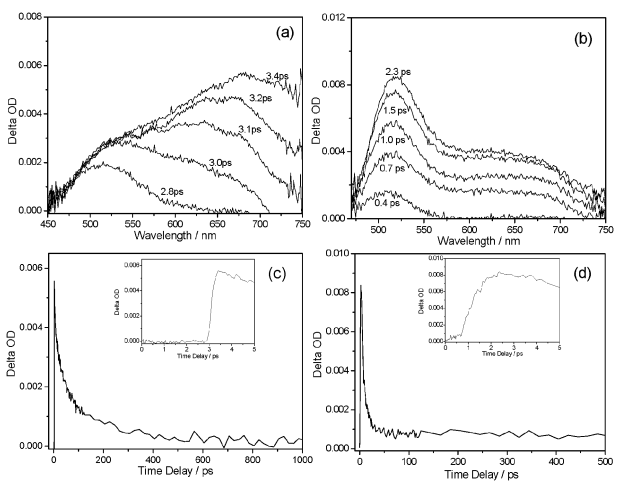

Fig. 6 Femtosecond TA spectra (a) and decay profile (c) with an inset of 5 ps window for bulk TiO_2 film in MeCN, and femtosecond TA spectra (b) and decay profile (d) with an inset of 5 ps window for MO in MeCN. Pump by 267 nm, probe at 675 nm.

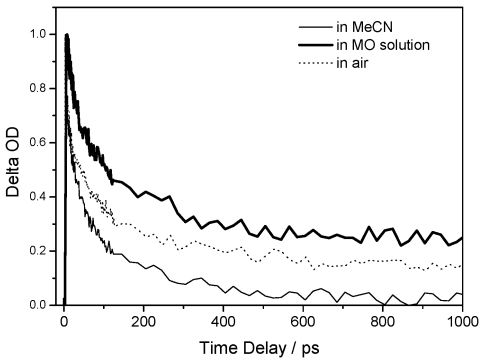

Fig. 7 TA decay profiles (normalized) of bulk TiO_2 film in MO solution, in MeCN, and in air, respectively. Pump by 267 nm, probe at 675 nm.

alcohols such as methanol and ethanol[26] which can scavenge holes on the picosecond time scale. This suggests that on the picosecond time scale, MO has no appreciable hole-scavenging effect and therefore the reaction between MO and electrons in the bulk TiO_2 film may be selectively observed through femtosecond TA measurement. Fig. 7 shows the TA decay profiles of bulk TiO_2 film in MO solution, in MeCN, and in air, respectively. MO has a weak TA at 675 nm whose onset and maximum are at 0.7 ps and 2.3 ps (Fig. 6(d), inset), earlier than the TA onset time (3.0 ps) of the bulk TiO_2 film (Fig. 6(c), inset). In order to get rid of the TA contribution from MO, the TA decay values of the bulk TiO_2 film in MO solution were subtracted by the MO TA decay values scaled by an appropriate factor (see Fig. S2 (ESI†) for details). From Fig. 7 it can be seen that the TA decay of bulk TiO_2 film in air and in MO solution is slower than that in pure MeCN and their Delta OD value does not decay to zero within 1000 ps (about 30% remained in MO solution). This phenomenon can be accounted for by electrons being consumed by oxygen and MO, resulting in holes left in TiO_2. This verifies that other than recombining with the holes in bulk TiO_2 film, the ultra fast free electrons can react with the organic dyes nearby on the order of picoseconds. In addition, it was found that MO has a more efficient capture effect of electrons than air as shown in Fig. 7.

It is commonly thought that in nano-sized TiO_2 almost all of the holes are trapped holes and a portion of the electrons are trapped electrons, both of which are localized at the surface of the nano-particles reacting with adsorbates on time scales ranging from microseconds to picoseconds.[25,26,30] Free electrons are distributed in the inner part of the nano-particles which would not react directly with surface adsorbates but can be stepwise trapped at the surface trap sites on the time scale between microseconds and milliseconds.[25] In bulk TiO_2 film it appears that most photo-generated electrons are free ones and they spread both in the inner part and on the surface. The electrons can directly react with MO and the remaining holes surviving to the nanosecond time scale can also oxidize MO. Concerning the particle size, the smaller the TiO_2 particle size, the lower the chance of recombination between the electrons and the holes. This leads to the photo-catalytic activity being improved,[33] accounting for why MO on nano-sized TiO_2 decomposes faster than that on bulk TiO_2 film. For treating a MO pollutant, usually nano-sized TiO_2 is used. In this case,

most electrons are spread in the inner part of the particles. On the particle surface, the trapped electrons are not as reductive as free electrons and may not be scavenged by MO. Therefore, in nano-sized TiO_2 the reactive species decomposing MO seems to be the holes through nanosecond time scale reaction. Although bulk TiO_2 film is not often applied in industry for MO degradation, it has the ability to decompose this dye through the reactive free electrons on the picosecond time scale.

Conclusions

The charge transfer process between MO molecules and bulk TiO_2 film and nano-sized TiO_2 was studied using TCSPC and nanosecond and femtosecond transient absorption spectroscopies. The recombination of electrons and holes in the bulk TiO_2 film occurs 1000 times faster than that in nano-sized TiO_2 particles. This can be attributed to the bulk TiO_2 film becoming a developed crystal that has fewer trapping sites to hinder the electrons and holes recombination. Unlike the broad TA spectra of nano-sized TiO_2 in the visible range, the bulk TiO_2 film exhibits two sharp and slightly red-shifted peaks at 520 nm and 675 nm. This appears due to that the nano-sized TiO_2 has its trapped electrons and holes spread broadly at a certain depth whereas in the bulk TiO_2 film most of the holes are shallowly trapped and a small part of them are deeper trapped ones. Both nano-sized TiO_2 and bulk TiO_2 film can directly decompose MO dye without the aid of radicals. In the nano-sized TiO_2 system, the trapped holes are consumed by MO in several hundreds of nanoseconds. In the bulk TiO_2 film, electrons are observed to inject into MO in several hundreds of picoseconds. Through cyclic voltammetry measurements, MO can be reduced at -0.28 V and oxidized at 1.4 V (*vs.* SCE), providing thermodynamic evidence for MO to be degraded by electrons and holes in TiO_2. In waste water treatment by nano-sized TiO_2, the competition between the holes of TiO_2 and the $OH^{\bullet}$ radicals towards decomposing MO depends on the concentration of MO. When MO is above 1.6×10^{-4} M, the degradation is mainly due to a direct hole oxidation process, while below 1.6×10^{-4} M, hydroxyl oxidation competes strongly and might exceed the direct hole oxidation.

Acknowledgements

This work was supported by a grant from the Research Grants Council of Hong Kong (HKU 7039/07P and HKU 7005/08P) and the University Grants Committee Special Equipment Grant (SEG-HKU-07). Support from the University Grants Committee, Areas of Excellence Scheme (AoE/P-03/08) is also gratefully acknowledged. J. Xi is thankful for the support from the National Natural Science Foundation of China (20973099).

Notes and references

1 P. V. Kamat, *Chem. Rev.*, 1993, **93**, 267.
2 M. A. Fox and M. T. Dulay, *Chem. Rev.*, 1993, **93**, 341.
3 A. Hagfeldt and M. Gratzel, *Chem. Rev.*, 1995, **95**, 49.
4 B. O'Regan and M. Gratzel, *Nature*, 1991, **353**, 737.
5 A. Fujishima, X. Zhang and D. A. Tryk, *Surf. Sci. Rep.*, 2008, **63**, 515.
6 R. Selvin, H. Hsu, N. S. Arul and S. Mathew, *Sci. Adv. Mater.*, 2010, **2**, 58.
7 M. R. Hoffmann, S. T. Martin, W. Choi and D. W. Bahnemann, *Chem. Rev.*, 1995, **95**, 69.
8 A. Fujishima, T. N. Rao and D. A. Tryk, *J. Photochem. Photobiol., C*, 2000, **1**, 1.
9 D. Hufschmidt, L. Liu, V. Seizer and D. Bahnemann, *Water Sci. Technol.*, 2004, **49**, 135.
10 M. A. Grela, M. E. J. Coronel and A. J. Colussi, *J. Phys. Chem.*, 1996, **100**, 16940.
11 L. Z. Sun and J. R. Bolton, *J. Phys. Chem.*, 1996, **100**, 4127.
12 P. F. Schwarz, N. J. Turro, S. H. Bossmann, A. M. Braun, A.-M. A. A. Wahab and H. Dürr, *J. Phys. Chem. B*, 1997, **101**, 7127.
13 Y. Nosaka, S. Komori, K. Yawata, T. Hirakawa and A. Y. Nosaka, *Phys. Chem. Chem. Phys.*, 2003, **5**, 4731.
14 Y. Chen, S. Yang, K. Wang and L. Lou, *J. Photochem. Photobiol., A*, 2005, **172**, 47.
15 L. Andronic and A. Duta, *Mater. Chem. Phys.*, 2008, **112**, 1078.
16 S. Padmaja and S. A. Madison, *J. Phys. Org. Chem.*, 1999, **12**, 221.
17 E. Dvininov, U. A. Joshi, J. R. Darwent, J. B. Claridge, Z. Xu and M. J. Rosseinsky, *Chem. Commun.*, 2011, **47**, 881.
18 K. Dai, H. Chen, T. Peng, D. Ke and H. Yi, *Chemosphere*, 2007, **69**, 1361.
19 K. Hara, T. Horiguchi, T. Kinoshita, K. Sayama, H. Sugihara and H. Arakawa, *Sol. Energy Mater. Sol. Cells*, 2000, **64**, 115.
20 W. Li, D. Li, J. Xian, W. Chen, Y. Hu, Y. Shao and X. Fu, *J. Phys. Chem. C*, 2010, **114**, 21482.
21 A. Kathiravan, P. Sathish Kumar, R. Renganathan and S. Anandan, *Colloids Surf., A*, 2009, **333**, 175.
22 W. Zhang, N. Ganesh, P. C. Mathias and B. T. Cunningham, *Small*, 2008, **4**, 2199.
23 A. Fujishima and X. Zhang, *C. R. Chim.*, 2006, **9**, 750.
24 M. Murai, Y. Tamaki, A. Furube, K. Hara and R. Katoh, *Catal. Today*, 2007, **120**, 214.
25 T. Yoshihara, R. Katoh, A. Furube, Y. Tamaki, M. Murai, K. Hara, S. Murata, H. Arakawa and M. Tachiya, *J. Phys. Chem. B*, 2004, **108**, 3817.
26 Y. Tamaki, A. Furube, M. Murai, K. Hara, R. Katoh and M. Tachiya, *J. Am. Chem. Soc.*, 2006, **128**, 416.
27 A. Safrany, R. Gao and J. Rabani, *J. Phys. Chem. B*, 2000, **104**, 5848.
28 N. Serpone, D. Lawless, R. Khairutdinov and E. Pelizzetti, *J. Phys. Chem.*, 1995, **99**, 16655.
29 A. Furube, T. Asahi, H. Masuhara, H. Yamashita and M. Anpo, *J. Phys. Chem. B*, 1999, **103**, 3120.
30 A. Yamakata, T. Ishibashi and H. Onishi, *J. Phys. Chem. B*, 2001, **105**, 7258.
31 R. Chen, J. Wang, H. Wang, W. Yao and J. Zhong, *Solid State Sci.*, 2011, **13**, 630.
32 X. Chen and S. S. Mao, *Chem. Rev.*, 2007, **107**, 2891.
33 J. Schwitzgebel, J. G. Ekerdt, H. Gerischer and A. Heller, *J. Phys. Chem.*, 1995, **99**, 5633.